UNIVERSITY OF BIRMINGHAM

University of Birmingham

Design of modified 4 × 6 filtering butler matrix based on all-resonator structures

Shao, Qiang; Chen, Fu-chang; Wang, Yi; Chu, Qing-xin; Lancaster, Michael J.

Link to publication on Research at Birmingham portal

Design of Modified 4×6 Filtering Butler Matrix Based on All-Resonator Structures

Qiang Shao, Fu-Chang Chen, *Member*, *IEEE*, Yi Wang, *Senior Member*, *IEEE*, Qing-Xin Chu, *Fellow*, *IEEE* and Michael J. Lancaster, *Senior Member*, *IEEE*

Abstract—In this paper, two novel 4×6 filtering Butler matrices with uniform and non-uniform power distribution are proposed. The matrices, consisting of a network of coupled resonators and two phase shifters, provide power division and phase shift together with a bandpass transfer function. The analytical synthesis procedures for the 4×6 filtering Butler matrices is presented. To verify the concept experimentally, two 4×6 filtering Butler matrices, operating at 2.4 GHz, with uniform and non-uniform power distribution are designed, fabricated, and measured. Simulated and measured results are found to be in good agreement with each other. Multibeam antenna arrays are realized by using the Butler matrix and the theoretical analysis has been confirmed by measurements of multibeam antenna arrays, which show reduced sidelobe level.

Index Terms—Bandpass filter, Butler matrix, microstrip, switched-beam antenna.

I. INTRODUCTION

IN RECENT years, the switched-beam antenna has become of great interest as it can achieve higher spectral efficiency and enhance the capacity of wireless communication systems. The standard switched-beam antenna array generally consists of three parts: switches, a beam-forming network (BFN), and an antenna array [1]. The switches determine which port the signal will be input from. The signal is then split in the BFN with incremental phases generated at its outputs. Finally, the output signal feed into the antenna array. The BFN is the core part of the switched-beam antenna array as the main beam will point at different directions based on the signals generated by it. Except for the Blass matrix [2], which is a lossy one, there are other two kinds of popular BFNs. One such a BFN is the Nolen matrix [3] and several Nolen matrices have been demonstrated for narrow band applications [4]-[6]. Another popular BFN is the Butler matrix [7], which is the subject of this paper. Several Butler matrices have been proposed for switched-beam antenna arrays [8]-[11]. In practical use, additional bandpass filters may be cascaded before the switches, to suppress spurious modes of the resonators, as well as reducing the intermodulation products generated by the

Fig. 1. (a) Schematic of a resonator-based 180° hybrid coupler as a building block. (b) Diagram of the modified 4×6 Butler matrix.

amplifiers. In this paper, to reduce the size and volume of such a system, the BFN and bandpass filter are replaced by a new Butler matrix with an inherent bandpass filter function. Conventionally the Butler matrix consists of several hybrid couplers and phase shifters and [12]-[14] present detailed systematic design methods. Introducing filtering functions to the hybrid couplers provides frequency selectivity into the Butler matrix. In [15]-[20], work has been done to introduce filtering functions to the hybrid coupler. A novel class of waveguide Butler matrices with inherent bandpass filter transfer functions was presented in [21]; the application here was in multi-port distributed power amplifiers. For antenna arrays, a low sidelobe level (SLL) is highly desired and one of the most effective methods to reduce the SLL is to apply non-uniform power tapering [22]-[24]. Several Butler matrices and Nolen matrices with reduced SLL have been proposed in [25]-[30], however these do not contain implicit filtering.

Recently, the authors have presented a 2×4 filtering Butler matrix using coupled resonators [31]. As the electric and magnetic coupling only generate ±90° phase shift, the resultant Butler matrix only provided two phase increments

(a)

(b)

Fig. 2. (a) Coupling scheme of the modified 4 × 6 filtering Butler matrix. (b) Layout of the modified 4 × 6 filtering Butler matrix. (L_3 = 10.89, L_4 = 7.00, L_5 = 10.00, L_6 = 13.54, L_7 = 12.47, L_8 = 13.08, L_9 = 18.36, L_{10} = 10.00, L_{11} = 14.83, L_{12} = 11.48, L_{13} = 25.48, L_{14} = 21.45, L_{15} = 5.00, S_1 = 0.2, S_6 = 0.2, W_1 = 0.4, W_2 = 1.0, W_3 = 2.2, all in millimeters.).

(0° and 180°). To extend the number of ports and generate more switched beams is a significant design challenge. In this paper, prototypes of a 4 × 6 filtering Butler matrix with a new modified topology and both uniform and non-uniform power distribution are presented. The analytical synthesis procedures for the Butler matrices are detailed, and example 4 × 6 filtering microstrip Butler matrices are designed, fabricated, and measured.

The paper is organized as follows. The design procedure of the modified 4 × 6 filtering Butler matrix with uniform power distribution is given in Section II. In Section III, a novel 180° filtering hybrid coupler with non-uniform power distribution is proposed. By utilizing this cou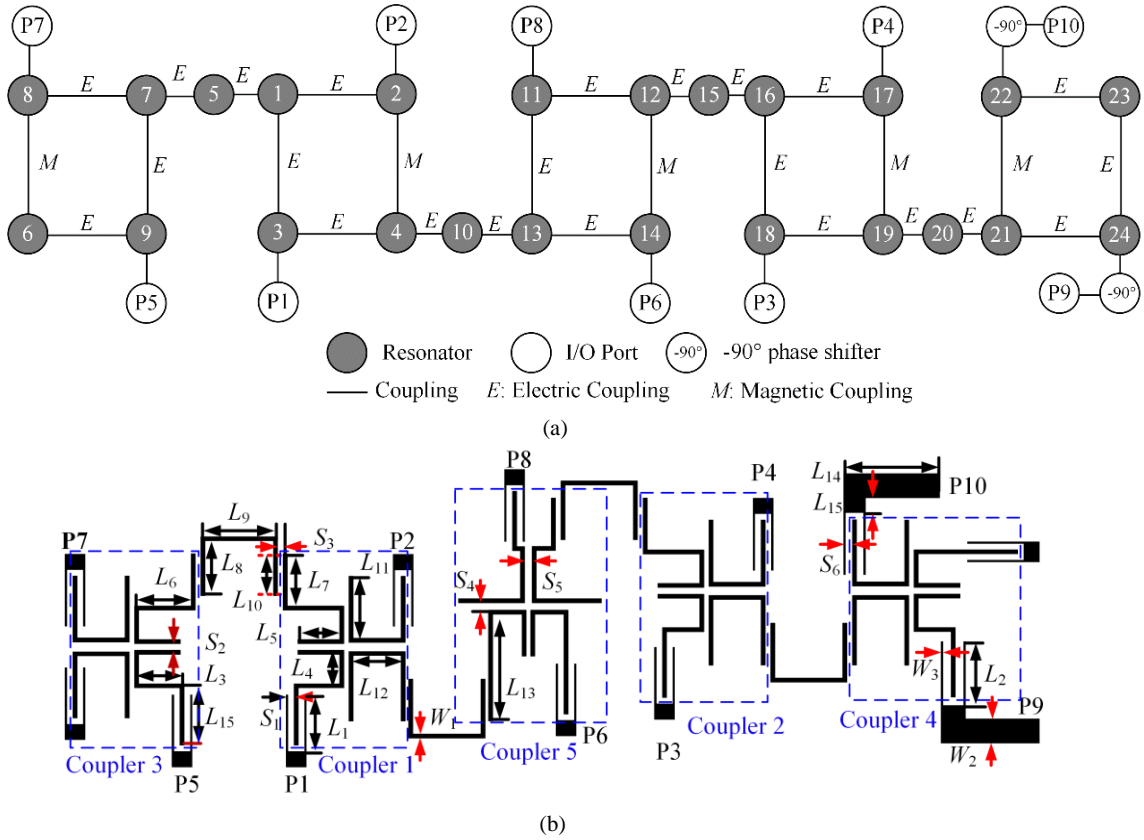pler, a modified 4 × 6 filtering Butler matrix with non-uniform power distribution is designed, fabricated and measured. Lastly, Section IV concludes this paper.

II. DESIGN OF MODIFIED 4 × 6 FILTERING WITH UNIFORM POWER DISTRIBUTION

A. Analysis

In our previous paper [29], a 180° filtering hybrid coupler, as shown in Fig. 1(a), was proposed. It is used in this paper as the building block of the new filtering Butler matrix. To realize the embedded filtering characteristic, the connecting network is formed of coupled resonators. However, this presents a problem with the implementation of the phase

shifter in the connecting network. To overcome this, a modified configuration of Butler matrix is shown in Fig. 1(b). Compared with the traditional topology of Butler matrix, an additional 180° hybrid coupler is introduced, and the phase shifter is moved from within the connecting network to the terminals. This facilitates the circuit implementation using resonators. However, in this case, there are six output ports but effectively only four are used. When using this matrix to feed a 4-element linear array as illustrated later in this paper, combining devices may be required in the final antenna system implementation, possibly with some impact on the RF performance. Fig. 2(a) and (b) show the coupling scheme of the modified 4 × 6 filtering Butler matrix and its microstrip layout on a substrate with a dielectric constant ε_r = 2.55, a loss tangent δ = 0.0029, and a thickness h = 0.8 mm. There are twenty-four resonators in the microstrip layout, each of which is a half-wavelength uniform impedance resonator and resonates at the central frequency of the bandpass filter (f_0). A 180° filtering hybrid coupler is composed of four resonators with an appropriate coupling scheme. The couplers are connected by direct coupling between resonators and the -90° phase shifters are realized by quarter-wavelength uniform impedance microstrip lines.

When port P1 or port P2 is the input port, based on the analysis in [29], the output ports P5, P6, P7, and P8 have equal amplitude and 0° or 180° phase shift. In this case the other ports are isolated. When port P3 is used as the input port, the
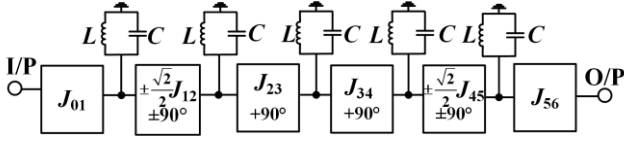
Fig. 3. Equivalent circuit of one signal path of the filtering Butler matrix.
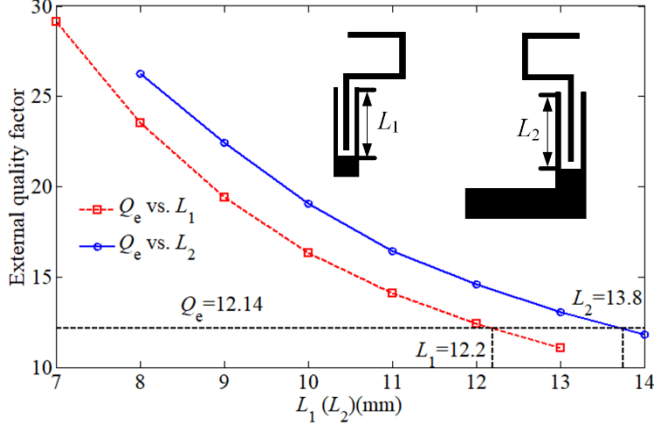

Fig. 4. Extracted resonators external quality factor with respect to the corresponding physical parameters.

phases of the output ports P6, P9, P8 and P10 can be calculated as

$$\angle S_{93} - \angle S_{63} = (\angle S_{C3} + \angle S_{DC} + \angle S_{9D})$$
$$- (\angle S_{A3} + \angle S_{BA} + \angle S_{6B})$$
$$= (\angle S_{C3} - \angle S_{A3}) + (\angle S_{DC} - \angle S_{BA}) \quad (1)$$
$$+ (\angle S_{9D} - \angle S_{6B})$$

$$\angle S_{83} - \angle S_{93} = (\angle S_{A3} + \angle S_{BA} + \angle S_{8B})$$
$$- (\angle S_{C3} + \angle S_{DC} + \angle S_{9D})$$
$$= (\angle S_{A3} - \angle S_{C3}) + (\angle S_{BA} - \angle S_{DC}) \quad (2)$$
$$+ (\angle S_{8B} - \angle S_{9D})$$

$$\angle S_{10,3} - \angle S_{83} = (\angle S_{C3} + \angle S_{DC} + \angle S_{10D})$$
$$- (\angle S_{A3} + \angle S_{BA} + \angle S_{8B})$$
$$= (\angle S_{C3} - \angle S_{A3}) + (\angle S_{DC} - \angle S_{BA}) \quad (3)$$
$$+ (\angle S_{10D} - \angle S_{8B})$$

where $\angle S_{ba}$ represents the phase response between the ports and the nodes A, B, C, D are defined in Fig. 1(b). Based on the properties of the 180° hybrid coupler, and taking the phase shift into account, the phase response across the output ports is

$$\angle S_{C3} = \angle S_{A3} \quad (4)$$

$$\angle S_{9D} - \angle S_{6B} = \angle S_{10D} - \angle S_{8B} = \angle S_{8B} - \angle S_{9D} = -90° \quad (5)$$

The modified 4×6 filtering matrix is realized by connecting the couplers together via AB and CD. These connections are simply made by coupling the resonators to the adjacent couplers as seen in Fig 2(a). The couplings are electrical, so the phase response of the connecting network is

$$\angle S_{DC} = \angle S_{BA} \quad (6)$$

Considering (1) to (6), when port P3 is used as the input port, the output phase increment can be calculated as

(a)

(b)
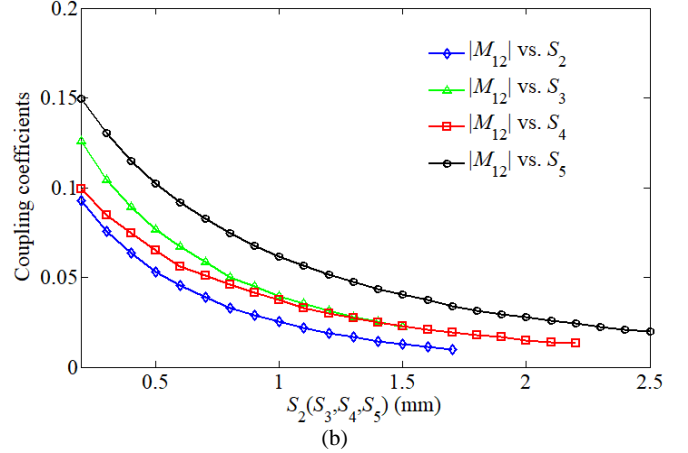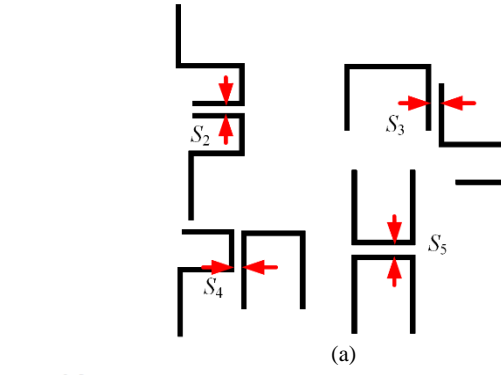
Fig. 5. (a) Circuit layout for extracting coupling coefficients $|M_{12}|$. (b) Extracted coupling coefficients with respect to the corresponding physical parameters.
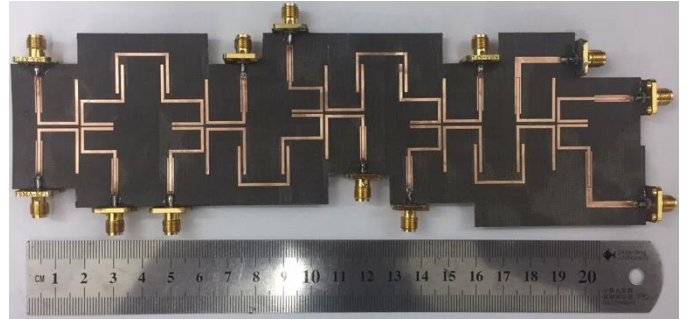
Fig. 6. Photograph of the fabricated modified 4×6 filtering Butler matrix.

$$\angle S_{93} - \angle S_{63} = \angle S_{83} - \angle S_{93} = \angle S_{10,3} - \angle S_{83} = -90° \quad (7)$$

In the same way, when port P4 is the input port, the output port phases can be calculated as

$$\angle S_{94} - \angle S_{64} = \angle S_{84} - \angle S_{94} = \angle S_{10,4} - \angle S_{84} = 90° \quad (8)$$

As in [29], the +90° admittance inverters J are used to model the input and output coupling. In Fig. 2(a) the +90° and -90° admittance inverters are used to represent the coupling dominated by electric fields and magnetic fields, respectively. Each path from an input port to an output port is equivalent to a fifth-order bandpass filter, as shown in Fig. 3; here the resonators are represented by parallel LC circuits. So the design can now follow that of a basic bandpass filter. Once the design requirements, such as the center frequency (f_0), fractional bandwidth (FBW) and ripple level are given, the element values (g_1, g_2, g_3, g_4, g_5) for the lowpass prototype
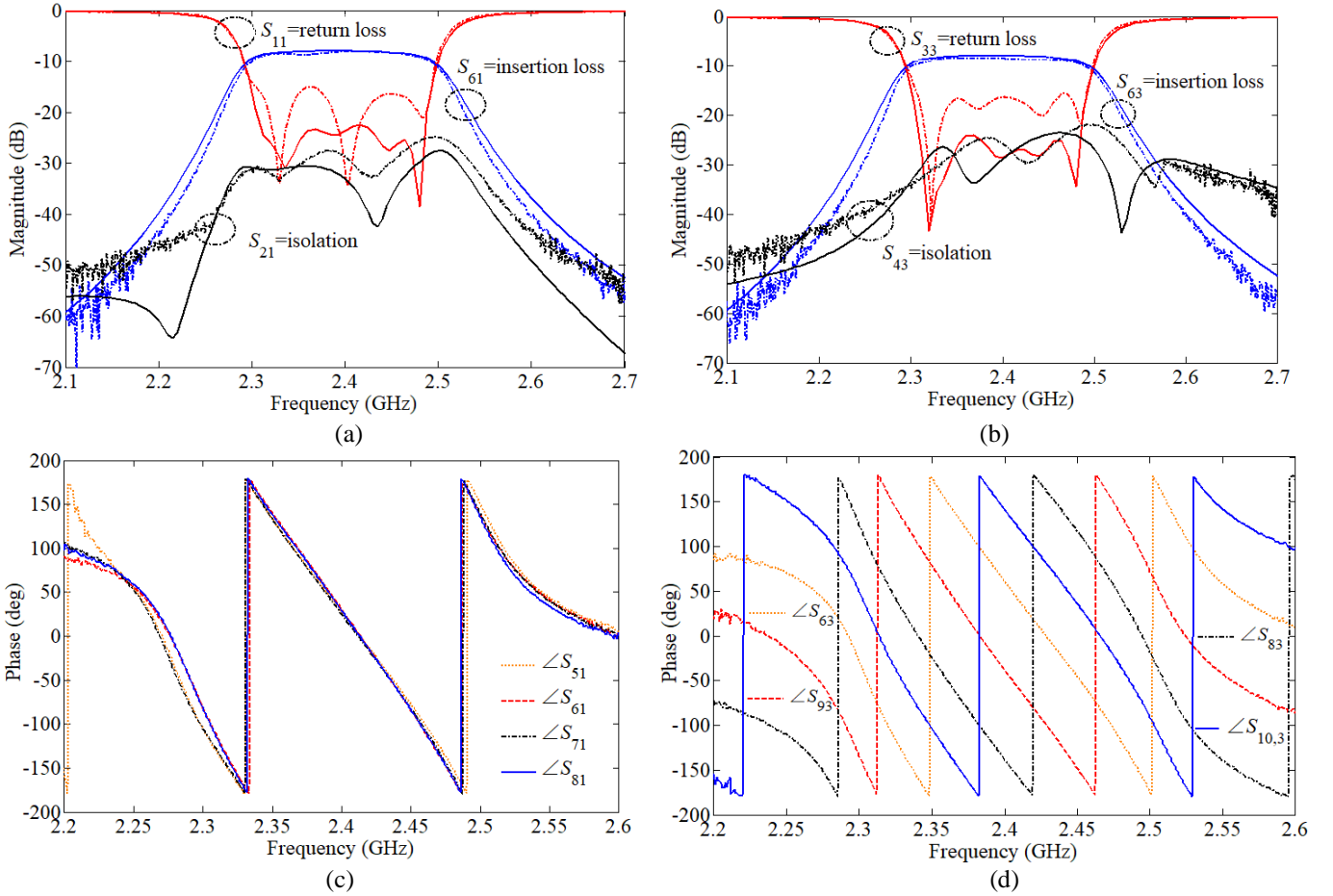
Fig. 7. Simulated and measured S-parameters of the fabricated 4×6 filtering Butler matrix. (solid lines: simulated results; dash-dotted lines: measured results). (a) S_{11}, S_{61}, and S_{21}. (b) S_{33}, S_{63}, and S_{43}. Measured output phases. (c) $\angle S_{51}$, $\angle S_{61}$, $\angle S_{71}$ and $\angle S_{81}$. (d) $\angle S_{63}$, $\angle S_{93}$, $\angle S_{83}$ and $\angle S_{10,3}$.

filter can be obtained, and then the bandpass coupling matrix design parameters can be calculated as follows [32]:

$$Q_{e1} = \frac{g_0 g_1}{FBW}, Q_{e2} = \frac{g_5 g_6}{FBW} \qquad (9)$$

$$M_{12} = \pm \frac{\sqrt{2}FBW}{2\sqrt{g_1 g_2}}, M_{23} = \frac{FBW}{\sqrt{g_2 g_3}}$$

$$M_{34} = \frac{FBW}{\sqrt{g_3 g_4}}, M_{45} = \pm \frac{\sqrt{2}FBW}{2\sqrt{g_4 g_5}} \qquad (10)$$

here Q_{e1} and Q_{e2} are the external quality factors of the resonators at the input and output, and $M_{12}, M_{23}, M_{34}, M_{45}$ are the coupling coefficients between the adjacent resonators ("+" denotes a coupling that is dominated by electric coupling, and "-" denotes one dominated by magnetic coupling).

B. Synthesis example

In order to verify the design concept, the new filtering Butler matrix has been designed, fabricated and measured. The center frequency of the filter is taken to be 2.4 GHz with a fractional bandwidth of 8%. The ripple level is 0.04321 corresponding to a 20 dB return loss. Therefore, the element values for the lowpass prototype filter are $g_1 = 0.9714$, $g_2 = 1.3721$, $g_3 = 1.8014$, $g_4 = 1.3721$ and $g_5 = 0.9714$. Based

on (9) and (10), the external quality factors can be calculated as $Q_{e1} = Q_{e2} = 12.14$ and the coupling coefficients between adjacent resonators are calculated as $M_{12} = M_{45} = \pm 0.049$ and $M_{23} = M_{34} = 0.050$.

Fig. 4 shows the extracted input and output resonators external quality factor with respect to the length of the feedlines (L_1 and L_2). These are obtained following the technique described in [32]. From the graph, the length of the feeding lines, for the required Q_e, can be obtained as $L_1 = 12.20$ mm and $L_2 = 13.80$ mm. These lengths are good initial values, but further optimization is required as described below. Similarly, the extracted coupling coefficients with respect to the gaps S_2, S_3, S_4 and S_5 are shown in Fig. 5 [32]. The initial values of the gaps between adjacent resonators can now be obtained as $S_2 = 0.54$ mm, $S_3 = 0.8$ mm, $S_4 = 0.72$ mm and $S_5 = 1.22$ mm. To improve the overall response, the initial dimensions of the gaps are optimized using IE3D software to be $L_1 = 12.20$ mm, $L_2 = 13.45$ mm, $S_2 = 0.56$ mm, $S_3 = 0.82$ mm, $S_4 = 0.71$ mm and $S_5 = 1.16$ mm. The small differences between the initial and optimized values show the excellent accuracy of the extraction technique.

C. Measurement results

Fig. 6 shows a photograph of the fabricated filtering Butler matrix. Fig. 7(a) and (b) show the simulated and measured S-

(a)   (b)   (c)
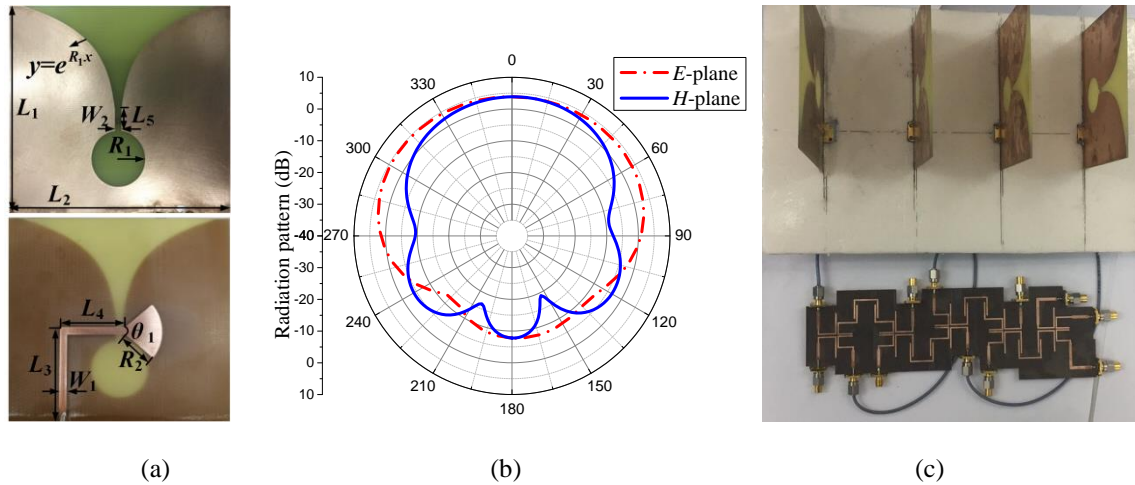
Fig. 8. (a) Antenna element. ($L_1 = 180.0$, $L_2 = 200.0$, $L_3 = 83.5$, $L_4 = 29.0$, $L_5 = 10.0$, $R_1 = 17.5$, $R_2 = 17.5$, $\theta_1 = 80°$, $W_1 = 1.5$, $W_2 = 1.5$, all in millimeters.)
(b) Simulated radiation patterns of the antenna element used in the linear array. (c) Prototype of the Butler matrix connected to the Vivaldi antenna array.

(a)

(b)

(c)

(d)
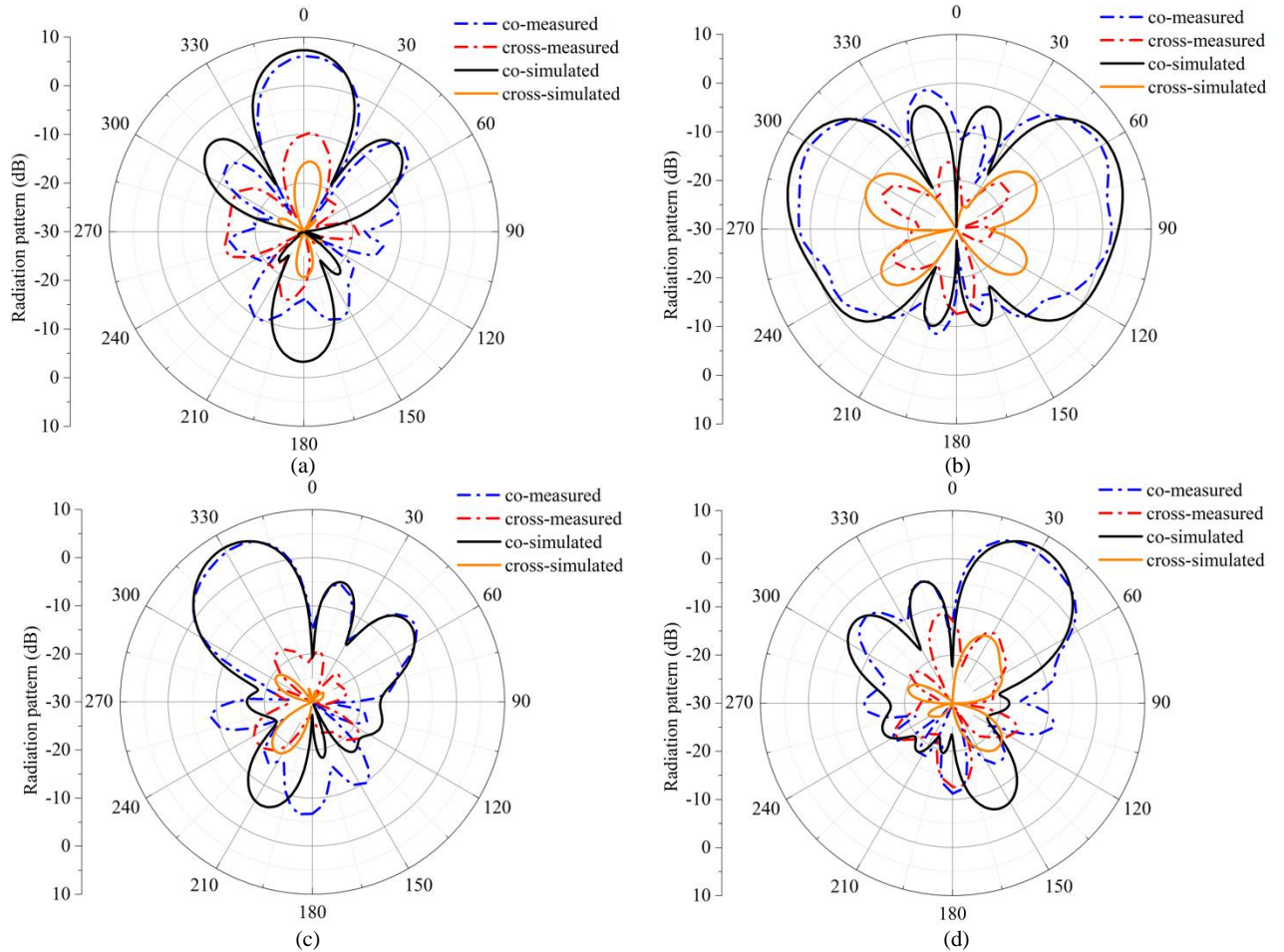
Fig. 9. Simulated and measured radiation patterns at 2.4 GHz when the input port is at (a) port P1; (b) port P2; (c) port P3; (d) port P4.

parameters when the signal is input at port P1 and port P3. The measured results are in good agreement with the simulated results. The measured minimum insertion loss for the bandpass filter is 8.9 dB, including the 6 dB power division and 2.9 dB filter loss. The return losses are higher than 15 dB. This deviation from 20 dB is likely caused by small errors in the structure dimensions. The measured isolation between port

P1 and port P2 and between port P3 and port P4 is larger than 22 dB in both cases. The measured output phases of the Butler matrix are shown in Fig. 7(c) and (d). As expected, $\angle S_{51}$, $\angle S_{61}$, $\angle S_{71}$ and $\angle S_{81}$ have equal phase and $\angle S_{63}$, $\angle S_{93}$, $\angle S_{83}$ and $\angle S_{10,3}$ have -90° phase shift. Over the 3-dB fractional bandwidth (2.3-2.5 GHz) of the filter, the measured phase imbalances are within ±10°.

(a)

(b)
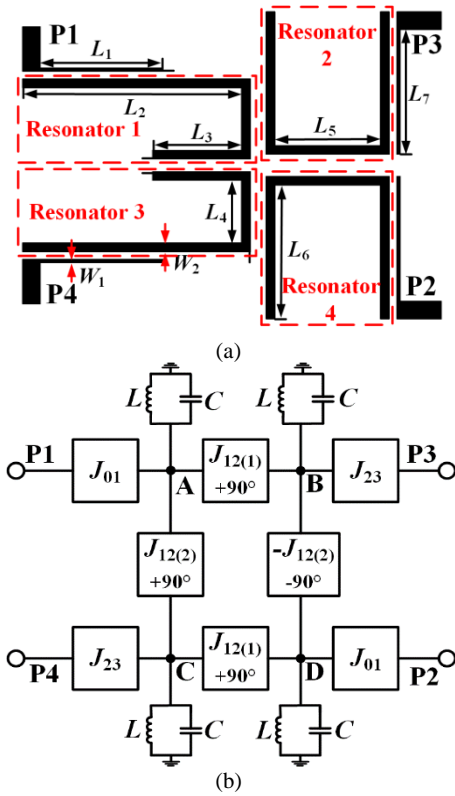
Fig. 10. (a) Layout of the 180° filtering hybrid coupler with unequal power ratio. (L_1 = 13.8, L_2 = 24.6, L_3 = 10.0, L_4 = 7.0, L_5 = 11.8, L_6 = 15.0, L_7 = 14.0, W_1 = 0.4, W_2 = 1.0, all in millimeters.) (b) Equivalent circuit of the 180° hybrid coupler with unequal power ratio.

(a)

(b)

(c)

(d)

Fig. 11. (a) Equivalent circuit of the 180° hybrid coupler from input port P1. (b) Equivalent circuit of a standard second-order coupled resonator bandpass filter. (c) Equivalent circuit of the 180° hybrid coupler between input port P1 and output port P3. (d) Equivalent circuit of the 180° hybrid coupler between input port P1 and output port P4.

D. Switched-beam antenna array

A switched-beam antenna array has been used to further test the filtering Butler matrix. The radiation element should have a broadband characteristic to cover the bandwidth of the bandpass filter, so a Vivaldi antenna is chosen. This is shown in Fig. 8(a). Four antenna elements have been equally spaced at a distance of 62.5 mm, which corresponds to 0.5 λ_0 at 2.4 GHz. The Butler matrix is connected to the antenna array via coaxial cables of equal-length, as shown in Fig. 8(b). It is worth mentioning that coaxial cables will need to be reconnected to the adequate antenna array elements when the input ports change from ports 1 and 2 to ports 3 and 4. The simulated and measured radiation patterns of the array obtained at 2.4 GHz are shown in Fig. 9. The directions of the main beams point at 0°, as shown in Fig. 9(a), when port P1 is used as the input port, whereas endfire performance is obtained when port P2 is the input port, as shown in Fig. 9(b). When port P3 and port P4 are used as the input port, the directions of the main beams point at -30° and +30°, as shown in Fig. 9(c) and (d) respectively. It can be seen that the measured results closely match the simulated results.

III. DESIGN OF 4 × 6 FILTERING BUTLER MATRIX WITH NON-UNIFORM POWER DISTRIBUTION

A. Analysis

In a practical application a low sidelobe level is important for the antenna array to select the desired signals. This can be
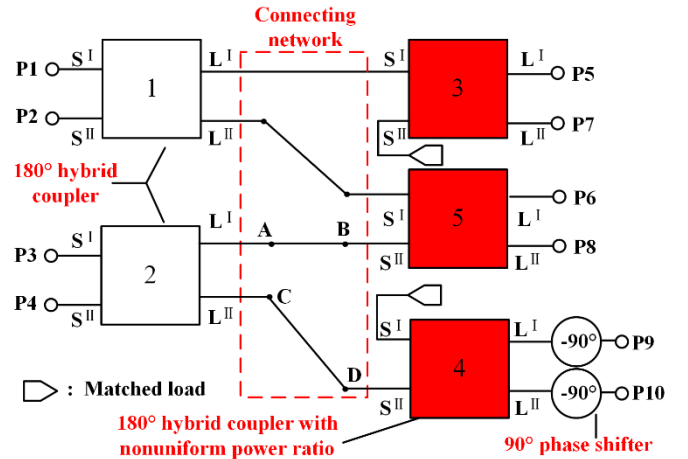
Fig. 12. The block diagram of the 4 × 6 Butler matrix with non-uniform power distribution by utilizing the 180° hybrid couplers.

achieved by a non-uniform power distribution of signals across the array. This section describes the design of a new 4 × 6 filtering Butler Matrix with non-uniform power distribution to achieve the desired level. A novel 180° filtering
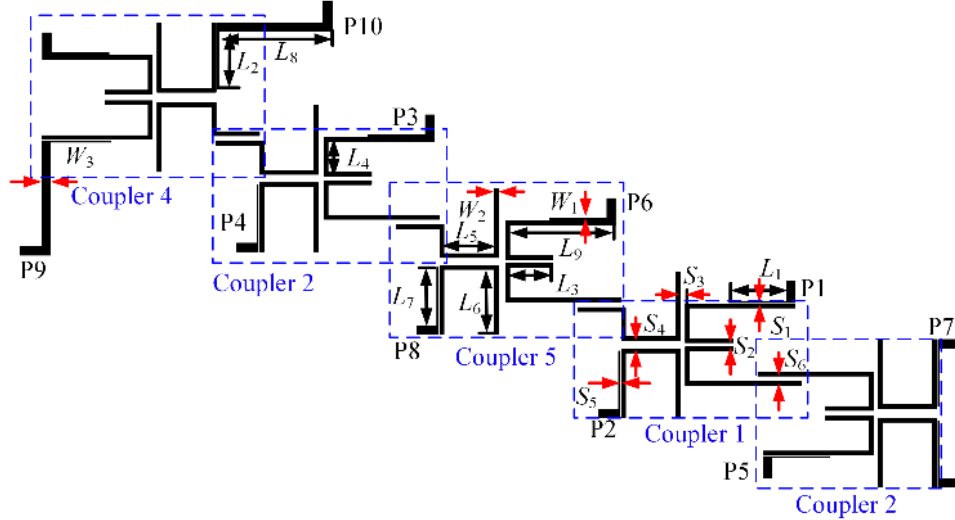
Fig. 13. Layout of the modified 4 × 6 filtering Butler matrix with non-uniform power distribution. ($L_3 = 10.00$, $L_4 = 7.00$, $L_5 = 11.53$, $L_6 = 15.00$, $L_7 = 13.50$, $L_8 = 26.10$, $L_9 = 24.29$, $S_1 = 0.25$, $S_5 = 0.25$, $W_1 = 0.4$, $W_2 = 1.0$, $W_3 = 2.2$, all in millimeters.)
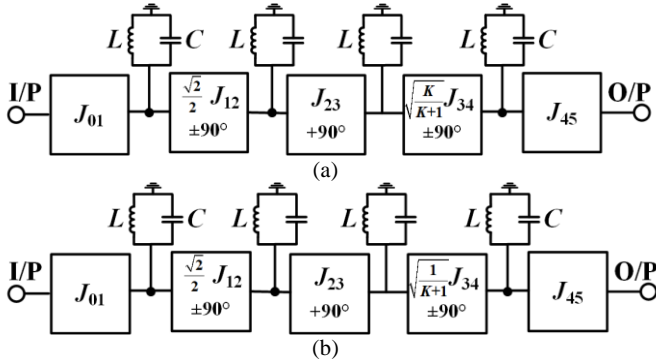
Fig. 14. Equivalent circuit of the 4 × 6 Butler matrix from the input port to output port with different power distribution. (a) K/(K+1); (b) 1/(K+1).

Fig. 15. Photograph of the fabricated 4 × 6 filtering Butler matrix with non-uniform power distribution.

hybrid coupler with unequal power distribution based on microstrip resonators is shown in Fig. 10(a). All the four microstrip resonators are half-wavelength uniform impedance resonators, which resonate at the central frequency of the filter. The input ports P1 and P2 are coupled to the resonators 1 and 4. The output ports P3 and P4 are coupled to the resonators 2 and 3. The coupling level between resonators 2 and 4 as well as between resonators 1 and 3 are equal in magnitude. So are the coupling level between resonators 1 and 2 and between resonators 3 and 4. However, the couplings between resonators 1 and 2, 1 and 3, 3 and 4 are dominated by the electric field, whereas the coupling between resonators 2 and 4 is dominated by the magnetic field. Different from the hybrid in [29], the coupling level between the resonators 1 and 2, and between resonators 1 and 3 are not identical. They control the power ratio of the output ports. This also applies to the coupling strengths between resonators 4 and 2 and between resonators 4 and 3.

Fig. 10(b) shows the equivalent circuit of the hybrid coupler. The coupling scheme of the coupler is the same as the 180° filtering hybrid coupler in [29], and therefore the output phase shifts remain unchanged. When the input signal is from port P1, the equivalent circuit is reduced to Fig. 11(a) because port P2 is isolated. The input admittance Y_{inA} from node A can be expressed as
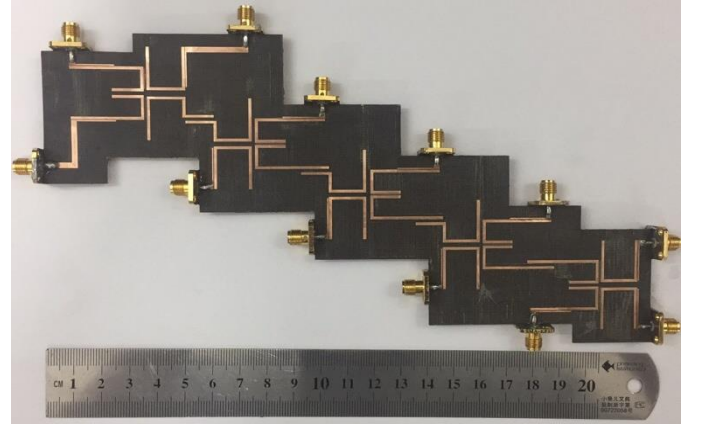
$$Y_{\mathrm{inA}} = \frac{J_{12(1)}^{\ 2}}{Y_{\mathrm{inB}}} + \frac{J_{12(2)}^{\ 2}}{Y_{\mathrm{inC}}} Y_{\mathrm{inA}} = \frac{J_{12(1)}^{\ 2}}{Y_{\mathrm{inB}}} + \frac{J_{12(2)}^{\ 2}}{Y_{\mathrm{inC}}} \qquad (11)$$

where Y_{inB} and Y_{inC} are the input admittance seen from node B and C. They can be expressed in turn as

$$Y_{\mathrm{inB}} = Y_{\mathrm{inC}} = \frac{J_{23}^{\ 2}}{Y_0} + j\omega C + \frac{1}{j\omega L} \qquad (12)$$

Hence the input admittance Y_{inA} becomes

$$Y_{\mathrm{inA}} = \frac{J_{12(1)}^{\ 2}}{Y_{\mathrm{inB}}} + \frac{J_{12(2)}^{\ 2}}{Y_{\mathrm{inC}}} = \frac{J_{12(1)}^{\ 2} + J_{12(2)}^{\ 2}}{Y_{\mathrm{inB}}} \qquad (13)$$

It can be seen that the equivalent circuit in Fig. 11(a) is a second-order bandpass filter as shown in Fig. 11(b), this then gives

$$J_{12(1)}^{\ 2} + J_{12(2)}^{\ 2} = J_{12}^{\ 2} \qquad (14)$$

where J_{12} is the inverter in the standard filter.

Now define K as the power ratio between the output port P3 and P4 when the input is at port P1. K can be expressed as [23]
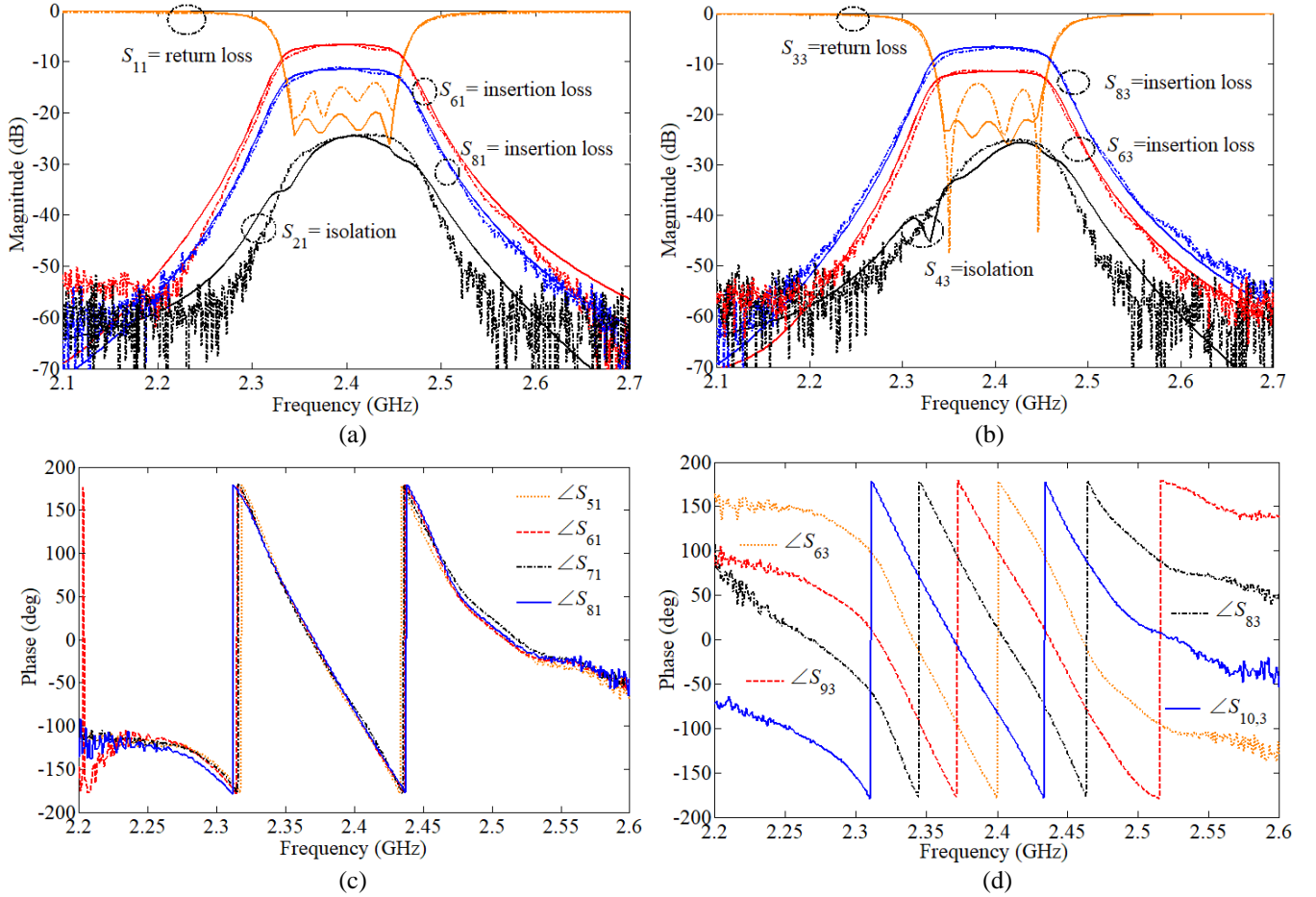
Fig. 16. Simulated and measured S-parameters of the fabricated modified 4 × 6 filtering Butler matrix with non-uniform power distribution. (solid lines: simulated results; dash-dotted lines: measured results). (a) S_{11}, S_{61}, and S_{21}. (b) S_{33}, S_{63}, and S_{43}. Measured output phases. (c) $\angle S_{51}$, $\angle S_{61}$, $\angle S_{71}$ and $\angle S_{81}$. (d) $\angle S_{63}$, $\angle S_{93}$, $\angle S_{83}$ and $\angle S_{10,3}$.

$$K = \frac{J_{12(1)}^{2}}{J_{12(2)}^{2}} \tag{15}$$

From (14) and (15), it can be found that

$$J_{12(1)} = \sqrt{\frac{K}{K+1}} J_{12}$$
$$J_{12(2)} = \sqrt{\frac{1}{K+1}} J_{12} \tag{16}$$

Therefore, the equivalent circuit of the 180° hybrid coupler from input port P1 to output ports P3 and P4 can be further reduced to the circuits in Fig. 11(c) and (d), respectively. The filter design parameters can be calculated as follows [32]

$$Q_{e1} = \frac{g_0 g_1}{FBW}, \quad Q_{e2} = \frac{g_2 g_3}{FBW} \tag{17}$$

$$M_{12(1)} = \sqrt{\frac{K}{1+K}} \frac{FBW}{\sqrt{g_1 g_2}}, \quad M_{12(2)} = \pm\sqrt{\frac{1}{1+K}} \frac{FBW}{\sqrt{g_1 g_2}}, \tag{18}$$

here Q_{e1} and Q_{e2} are the external quality factors of the resonators at the input and output, and $M_{12(1)}$ and $M_{12(2)}$ are the coupling coefficients between the adjacent resonators. By symmetry, when the signal is input from port P2, the power ratio of the output port P3 and port P4 is $1/K$.

To realize a 4 × 6 Butler matrix with non-uniform power distribution, the 180° filtering hybrid couplers connected to the output ports in Fig. 1(c) are replaced by the new couplers with unequal power ratio, as shown in Fig. 12. Fig. 13 shows the microstrip layout of the Butler matrix with non-uniform power distribution. Similar to the analysis in Section II, each path from an input to an output port can be equivalent to a fourth order bandpass filter as shown in Fig. 14. The bandpass design parameters can thus be calculated as [32]

$$Q_{e1} = \frac{g_0 g_1}{FBW}, Q_{e2} = \frac{g_4 g_5}{FBW} \tag{19}$$

$$M_{12} = \pm\frac{\sqrt{2}FBW}{2\sqrt{g_1 g_2}}, M_{23} = \frac{FBW}{\sqrt{g_2 g_3}} \tag{20}$$

$$M_{34(1)} = \sqrt{\frac{K}{1+K}} \frac{FBW}{\sqrt{g_3 g_4}}, M_{34(2)} = \pm\sqrt{\frac{1}{1+K}} \frac{FBW}{\sqrt{g_3 g_4}}$$

B. Synthesis example

In order to verify the design concept, a modified 4 × 6 filtering Butler matrix with output ports P5, P6, P7, P8 (or ports P6, P9, P8, P10) and power ratio of 1:3:3:1 is designed, fabricated and measured. The center frequency of the filter is taken to be 2.4 GHz with a fractional bandwidth of 4.5%. The
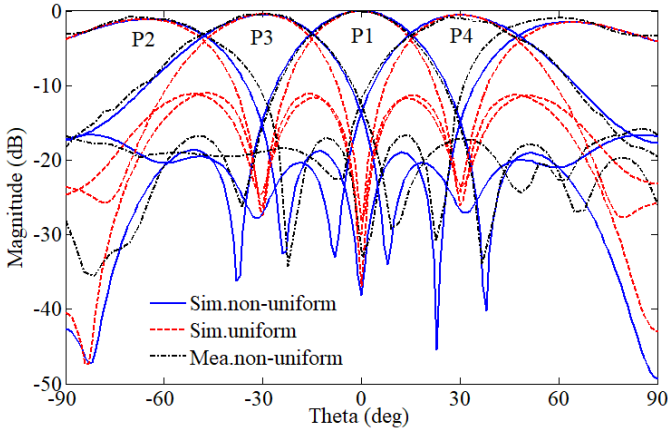
Fig. 17. Simulated and measured radiation patterns at 2.4 GHz when the input is at different ports.

ripple level is 0.04321. The element values can be obtained as $g_1 = 0.9314$, $g_2 = 1.2920$, $g_3 = 1.5775$, $g_4 = 0.7628$ and $g_5 = 1.2210$. Based on (19) and (20), the external quality factors can be easily calculated as $Q_{e1} = Q_{e2} = 20.7$ and the coupling coefficients between adjacent resonators are calculated as $M_{12} = \pm0.033$ and $M_{23} = 0.033$. For coupler 3 in Fig 12, the power ratio K_3 is required to be 1/3, so $M_{34(1)} = 0.021$ and $M_{34(2)} = 0.036$. For coupler 4, the power ratio is $K_4 = 1/3$, so $M_{34(1)} = 0.021$ and $M_{34(2)} = 0.036$ and for coupler 5 the power ratio should be $K_5 = 3$, so $M_{34(1)} = 0.036$ and $M_{34(2)} = 0.021$.

Using an extraction procedure similar to that in Section II, the initial values of the length of the feeding lines, for the required Q_e, can be obtained as $L_1 = 13.20$ mm and $L_2 = 13.80$ mm. The gaps between the adjacent resonators are $S_2 = 0.81$ mm, $S_3 = 1.15$ mm, $S_4 = 1.85$ mm, $S_6 = 1.20$ mm, $S_7 = 0.75$ mm, $S_8 = 1.59$ mm, $S_9 = 1.74$, $S_{10} = 1.12$ mm, $S_{11} = 1.10$ mm and $S_{12} = 2.38$ mm according to the design curves in Fig. 5. The final dimensions of the gaps in Fig. 13 are optimized using IE3D software to be $L_1 = 13.28$ mm, $L_2 = 13.78$ mm, $S_2 = 0.91$ mm, $S_3 = 1.23$ mm, $S_4 = 1.67$ mm, $S_6 = 1.23$ mm, $S_7 = 0.75$ mm, $S_8 = 1.65$ mm, $S_9 = 1.67$, $S_{10} = 1.27$ mm, $S_{11} = 1.06$ mm and $S_{12} = 2.35$ mm. Again, the small difference in the values after optimization indicate the accuracy of the technique.

C. Measurement results

Fig. 15 shows a photograph of the fabricated Butler matrix. Measurements have been done taking the input ports P1 and P3 as an example. The simulated and measured S-parameters of the fabricated Butler matrix are shown in Fig. 16(a) and (b). For the low power path, the measured minimum insertion loss is 11.8 dB, including the 9 dB power division and 2.8 dB filter loss. For the high power path, the measured minimum insertion loss is 7.2 dB, including the 4.3 dB power division and 2.9 dB filter loss. The measured return losses are higher than 14 dB and the isolation between port P1 and port P2 (or port P3 and port P4) is larger than 25 dB. The measured output phases of the fabricated non-uniform filtering Butler matrix are shown in Fig. 16(c) and (d). When the input signal is from port P1, the phases $\angle S_{51}$, $\angle S_{61}$, $\angle S_{71}$ and $\angle S_{81}$ are almost equal. When the input signal is from port P3, the phases $\angle S_{63}$, $\angle S_{93}$, $\angle S_{83}$ and $\angle S_{10,3}$ are around -90°. Over the 3-dB fractional bandwidth (2.34-2.46 GHz) of the bandpass filter, all the measured phase imbalances are within ± 9°.

Again, a Vivaldi antenna array has been used to further test the filtering Butler matrix. The simulated and measured radiation patterns of the Vivaldi antenna array obtained at 2.4 GHz are shown in Fig. 17. This is a linear plot for clearer comparison. As expected, the main beams angles are 0°, 180°, -30°, +30° when the input is at port P1, P2, P3, P4 respectively. More importantly, Fig 17 shows that with the non-uniform power excitation, the measured sidelobe levels have been reduced from -10 dB to -15 dB. Good agreement has been obtained between the simulated and measured results.

IV. CONCLUSION

A systematic design procedure of two modified 4×6 filtering Butler matrices with uniform and non-uniform power distribution have been presented in this paper. The Butler matrix is composed of coupled resonators and phase shifters, providing power division, phase shift and a bandpass response. By controlling the coupling between resonators in the couplers, a 4×6 filtering Butler matrix with non-uniform power distribution has been designed to suppress side lobe levels. For validation, two 4×6 filtering Butler matrices with uniform and non-uniform power distribution have been designed, fabricated and measured. In addition, a Vivaldi antenna array was used to examine the radiation performance of the new Butler matrix design. Close correlation between the simulated and measured results confirms the effectiveness of the design method. It is worth mentioning that in this paper a single layer substrate is used, this leads to output ports locations in the same plane. A conventional Butler matrix has another crossing layer before the output ports which may lead to more flexibly in port location.

REFERENCES

[1] T.-H. Lin, S.-K. Hsu, and T.-L. Wu, "Bandwidth enhancement of 4×4 Butler matrix using broadband forward-wave directional coupler and phase difference compensation," *IEEE Trans. Microw. Theory Techn.*, vol. 61, no. 12, pp. 4099–4109, Dec. 2013.

[2] J. Blass, "Multidirectionnal antenna, a new approach to stacked beams," *IRE Int. Conf. Record*, vol. 8, pt. 1, pp. 48–50, 1960.

[3] J. Nolen, "Synthesis of multiple beam networks for arbitrary illuminations," Ph.D. dissertation, The Johns Hopkins Univ., Baltimore, MD, 1965.

[4] N. Fonseca, "Printed S-band 4×4 Nolen matrix for multiple beam antenna applications," *IEEE Trans. Antennas Propag.*, vol. 57, no. 6, pp. 1673-1678, Jun. 2009.

[5] T. Djerafi, N. Fonseca, and K. Wu, "Planar Ku-band 4×4 Nolen matrix in SIW technology," *IEEE Trans. Microw. Theory Techn.*, vol. 58, no. 2, pp. 259-266, Feb. 2010.

[6] T. Djerafi, N. Fonseca, and K. Wu, "Broadband substrate integrated waveguide 4×4 Nolen matrix based on coupler delay compensation," *IEEE Trans. Microw. Theory Techn.*, vol. 59, no. 7, pp. 1740-1745, Jul 2011.

[7] J. Butler and R. Lowe, "Beam-forming matrix simplifies design of electronically scanned antennas," *Electron. Design*, pp. 170–173, Apr. 1961.

[8] Q.-P. Chen, Z, Qamar, S.-Y. Zheng, Y. Long and D. Ho, "Design of a compact wideband butler matrix using vertically installed planar structure," *IEEE Trans. Compon. Packag. Manuf. Technol.*, vol. 8, no. 8, pp. 1420 - 1430, Aug 2018.

[9] K. Wincza and S. Gruszczynski, "Broadband integrated 8 × 8 Butler matrix utilizing quadrature couplers and Schiffman phase shifters for multibeam antennas with broadside beam", *IEEE Trans. Microw. Theory Techn.*, vol. 64, no. 8, pp. 2596-2604, Aug. 2016.

[10] K. Wincza, K. Staszek, and S. Gruszczynski, "Broadband multibeam antenna arrays fed by frequency-dependent butler matrices," *IEEE Trans. Antennas Propag.*, vol. 65, no. 9, pp. 4539 - 4547, Sep. 2017.

[11] Y. Cao, K.-S. Chin, W.-Q. Che, W.-C. Yang, and E. S. Li, "A compact 38 GHz multibeam antenna array with multifolded butler matrix for 5G applications," *IEEE Antennas Wireless Propag. Lett.*, vol. 16, pp. 2996 - 2999, 2017.

[12] J. Allen, "A theoretical limitation on the formation of lossless multiple beams in linear arrays," *IEEE Trans. Antennas Propag.*, vol. 9, no. 4, pp. 350–352, Jul. 1961.

[13] H. Moody, "The systematic design of the Butler matrix," *IEEE Trans. Antennas Propag.*, vol. 12, no. 6, pp. 786–788, Nov. 1964.

[14] M. Ueno, "A systematic design formulation for Butler matrix applied FFT algorithm," *IEEE Trans. Antennas Propag.*, vol. 29, no. 3, pp. 496–501, May 1981.

[15] C.-K. Lin and S.-J. Chung, "A compact filtering 180 hybrid," *IEEE Trans. Microw. Theory Techn.*, vol. 59, no. 12, pp. 3030–3036, Dec. 2011.

[16] L.-S. Wu, B. Xia, W.-Y. Yin, and J. Mao, "Collaborative design of a new dual-bandpass 180° hybrid coupler," *IEEE Trans. Microw. Theory Techn.*, vol. 61, no. 3, pp. 1053–1066, Mar. 2013.

[17] U. Rosenberg, M. Salehi, S. Amari, and J. Bornemann, "Compact multi-port power combination/distribution with inherent bandpass filter characteristics," *IEEE Trans. Microw. Theory Techn.*, vol. 62, no. 11, pp. 2659–2672, Nov. 2014.

[18] T. Skaik, M. Lancaster, and F. Huang, "Synthesis of multiple output coupled resonator circuits using coupling matrix optimisation," *IET Microw. Antennas Propag.*, vol. 5, no. 9, pp. 1081–1088, 2011.

[19] F. Lin, Q. X. Chu, and S. W. Wong, "Design of dual-band filtering quadrature coupler using and resonators," *IEEE Microw. Wireless Compon. Lett.*, vol. 22, no. 11, pp. 565–567, Nov. 2012.

[20] K. Song, X. Ren, F. Chen, and Y. Fan, "Compact in-phase power divider integrated filtering response using spiral resonator," *IET Microw. Antennas Propag.*, vol. 8, no. 4, pp. 228–234, Mar. 2014.

[21] V. T. Crestvolant, P. M. Iglesias, and M. J. Lancaster, "Advanced Butler matrices with integrated bandpass filter functions," *IEEE Trans. Microw. Theory Techn.*, vol. 62, no. 11, pp. 2659–2672, Nov. 2014.

[22] S.-J. Park, D.-H. Shin, and S.-O. Park, "Low side-lobe substrate integrated-waveguide antenna array using broadband unequal feeding network for millimeter-wave handset device," *IEEE Trans. Antennas Propag.*, vol. 64, no. 3, pp. 923–932, Mar. 2016.

[23] F. C. Chen, H. T. Hu, R. S. Li, Q. X. Chu, and M. J. Lancaster, "Design of filtering antenna array with reduced sidelobe level," *IEEE Trans. Antennas Propag.*, vol. 65, no. 2, pp. 903–908, Feb. 2017.

[24] L. Chang, Y. Li, Z. Zhang, X. Li, S. Wang, and Z. Feng, "Low-sidelobe air-filled slot array fabricated using silicon micromachining technology for millimeter-wave application," *IEEE Trans. Antennas Propag.*, vol. 65, no. 8, pp. 4067–4074, Aug. 2017.

[25] J. Shelton, "Reduced sidelobes for Butler-matrix-fed linear arrays," *IEEE Trans. Antennas Propag.*, vol. AP-17, no. 5, pp. 645–647, Sep. 1969.

[26] K. Wincza, S. Grunszczynski, and K. Sachse, "Reduced sidelobe four-beam antenna array fed by modified butler matrix," *Electron. Lett.*, vol. 42, no. 9, pp 508-509, Apr. 2006.

[27] K. Tekkouk, J. Hirokawa, R. Sauleau, M. Ettorre, M. Sano, and M. Ando, "Dual-layer ridged waveguide slot array fed by a Butler matrix with sidelobe control in the 60-GHz band," *IEEE Trans. Antennas Propag.*, vol. 63, no. 9, pp. 3857–3867, Sep. 2015.

[28] J. W. Lian, Y. L. Ban, C. H. Xiao, and Z. F. Yu, "Compact substrate-integrated 4 × 8 Butler matrix with sidelobe suppression for millimeter-wave multibeam application," *IEEE Antennas Wireless Propag. Lett.*, vol. 17, no. 5, pp. 928–932, May 2018.

[29] N. Fonseca and N. Ferrando, "Nolen matrix with tapered amplitude law for linear arrays with reduced side lobe level," in *Proc. Eur. Conf. Antennas Propag.*, Barcelona, Spain, Apr. 2010.

[30] I. Slomian, K. Wincza, and S. Gruszczynski, "Circularly polarized switched-beam antenna arrays with reduced sidelobe level," *IEEE Antennas Wireless Propag. Lett.*, vol. 15, pp. 1213–1216, 2016.

[31] Q. Shao, F. C. Chen, Q. X. Chu, and M. J. Lancaster, "Novel filtering 180° hybrid coupler and its application to 2 × 4 filtering Butler matrix,"

[   ] *IEEE Trans. Microw. Theory Techn.*, vol. 66, no. 7, pp. 3288–3296, Jul. 2018.

[32] J. S. Hong and M. J. Lancaster, *Microstrip Filters for RF/Microwave Applications*. New York, NY, USA: Wiley, 2001.

Qiang Shao was born in Xianning, Hubei Province, China, in January 1993. He received the B.S. degree in information engineering from Shantou University, Shantou, Guangdong, China in 2015. He is currently working towards the Ph.D. degree at South China University of Technology. His research interests include microwave filters and associated RF circuits for microwave and millimeter-wave applications.

Fu-Chang Chen (M'12) was born in Fuzhou, Jiangxi Province, China, in December 1982. He received the Ph.D. degree from South China University of Technology, Guangzhou, Guangdong, China, in 2010. He is currently a Professor with the School of Electronic and Information Engineering, South China University of Technology. His research interests include the synthesis theory and design of microwave filters and associated RF modules for microwave and millimeter-wave applications.

Yi Wang (M'09–SM'12) was born in Shandong, China. He received the B.Sc. degree in physics and M.Sc. degree in condensed matter physics from the University of Science and Technology, Beijing, China, in 1998 and 2001, respectively, and the Ph.D. degree in electronic and electrical engineering from the University of Birmingham, Edgbaston, Birmingham, U.K., in 2005. In 2011, he became a Senior Lecturer and then Reader at the University of Greenwich. In 2018, Yi joined Birmingham as a Senior Lecturer. His current research interests include millimeter-wave and terahertz devices for metrology, communications and sensors, micromachining, microwave circuits based on multiport filtering networks, and filter-antenna integration.

Qing-Xin Chu (M'99–SM'11–F'18) received the B.S., M.E., and Ph.D. degree in electronic engineering from Xidian University, Xi'an, Shaanxi, China, in 1982, 1987, and 1994, respectively.

He is currently a chair professor with the School of Electronic and Information Engineering, South China University of Technology. He is also the director of the Research Institute of Antennas and RF Techniques of the university, the chair of the Engineering Center of Antennas and RF Techniques of Guangdong Province. He is also with Xidian University as a distinguished professor in Shaanxi Hundred-Talent Program since 2011. From Jan. 1982 until Jan. 2004, he was with the School of Electronic Engineering, Xidian University, and since 1997, he was a professor and the vice dean of the School of Electronic Engineering, Xidian University.

He is the foundation chair of IEEE Guangzhou AP/MTT Chapter, the senior members of IEEE and the China Electronic Institute (CEI). He has published over 300 papers in journals and conferences, which were indexed in SCI more than 1500 times. One of his papers published in IEEE Transactions on Antennas and Propagations in 2008 becomes the top ESI (Essential Science Indicators) paper within 10 years in the field of antenna (SCI indexed self-excluded in the antenna field ranged top 1%). In 2014, he was elected as the highly cited scholar by Elsevier in the field of Electrical and Electronic Engineering. He has authorized more than 30 invention patents of China.

He was the recipient of the Science Award by Guangdong Province in 2013，the Science Awards by the Education Ministry of China in 2008 and 2002, the Fellowship Award by Japan Society for Promotion of Science (JSPS) in 2004, the Singapore Tan Chin Tuan Exchange Fellowship Award in 2003, the Educational Award by Shaanxi Province in 2003.

His current research interests include antennas in wireless communication, microwave filters, spatial power combining array, and numerical techniques in electromagnetics.

Michael J. Lancaster (M'91–SM'04) was born in Keighley, Yorkshire, U.K., in 1958. He received the B.Sc. degree in physics and Ph.D. degree from Bath University, Bath, U.K., in 1980 and 1984, respectively. His doctoral research focused on nonlinear underwater acoustics.

Upon leaving Bath University, he joined the Surface Acoustic Wave (SAW) Group, Department of Engineering Science, Oxford University, Oxford, U.K., as a Research Fellow, where his research concerned the design of new novel surface acoustic wave (SAW) devices including filters and filter banks. In 1987, he became a Lecturer with the Department of Electronic and Electrical Engineering, University of Birmingham, Birmingham, U.K., where he lectures on electromagnetic theory and microwave engineering. Shortly after he joined the department, he began the study of the science and applications of high-temperature superconductors, working mainly at microwave frequencies. In 2000, he became Head of the Emerging Device Technology Research Centre, and in 2003, Head of the Department of Electronic, Electrical and Computer Engineering. He has authored or coauthored over 170 papers in refereed journals and 2 books. His current personal research interests include microwave filters and antennas, as well as the high-frequency properties and applications of a number of novel and diverse materials.

Prof. Lancaster is Fellow of the IET and U.K. Institute of Physics. He is a Chartered Engineer and Chartered Physicist. He has served on the IEEE Microwave Theory and Techniques (IEEE MTT-S) International Microwave Symposium (IMS) Technical Committee.